PAR ELEVATION INFLUENCE ON HYDROGEN FLOOR LAYER DEPTH

F. Dabbene

CEA, DEN, DANS/DM2S/SFME/LTMF - F-91191 Gif-sur-Yvette Cedex, France.

Abstract

In order to circumvent problems associated with containment loads resulting from a possible hydrogen combustion, French containments for instance are equipped with passive autocatalytic recombiners (PAR). The aim of this safety device is to recombine hydrogen with oxygen in order to limit hydrogen concentration. Hence, PAR distribution within the containment is a key feature to limit the hydrogen risk. According with the PARIS benchmark scenario and boundary conditions therein (EU-FP6, SARNET project) a floor layer developed with low mass and thermal mixing processes. In this paper we illustrate the link between the PAR elevation and the floor layer depth.

Introduction

During the course of a severe accident in light water reactors, a large amount of hydrogen could be generated and accumulated in the containment atmosphere. There, hydrogen, air and steam mixed possibly creating local flammable conditions. In order to circumvent problems associated with containment loads resulting from a possible hydrogen combustion, French containments for instance are equipped with passive autocatalytic recombiners (PAR). The aim of this safety device is to recombine hydrogen with oxygen in order to limit hydrogen concentration.

Hence, PAR distribution within the containment is a key feature to limit the hydrogen risk. Thus, experimental and numerical tests were developed to better understand PAR behavior. Recently, the PARIS numerical benchmark was initiated in the frame of SARNET (Severe Accident Research Network of Excellence, project supported by the 6th Research

and Technology Framework Program developed by the European Commission). According with the PARIS scenario and boundary conditions therein, a floor layer developed with low mass and thermal mixing processes. In this paper we illustrate the link between the PAR elevation and the floor layer depth.

In the first section we describe the PAR black-box model and the in-house CAST3M/TONUS CFD code used in this study. In the second section, the PARIS benchmark and associated new cases are presented. At last, numerical results are compared for the different configurations.

1 Code and PAR model description

The CAST3M/TONUS code was developed by CEA and IRSN over the last decade, to model hydrogen release, distribution and combustion in a PWR reactor containment [1]. The code has both multi-compartment lumped parameter (LP) and computational fluid dynamics (CFD) formulations. Since the objective of the code is to be applied to real plant applications, numerical considerations such as mesh size and CPU run-time constrained the choice of physical models and numerical algorithms. It's why the PAR is considered as a black-box and connected to the CFD formulation according with appropriate boundary conditions.

1.1 General code description

Numerical algorithms suited to the various flow regimes — low Mach number flows characteristic of the hydrogen distribution phase up to high speed flows associated with hydrogen combustion [2, 3] — have been developed and optimized to perform efficiently on the single processor platforms (Linux or Windows PC) on which the CAST3M/TONUS code was developed.

For the distribution part, the low Mach number multi-component Navier-Stokes solver incorporates two types of turbulence models — mixing length and standard k- ϵ models — and wall condensation models based on the heat and mass transfer analogy — Chilton-Colburn correlations [4]. Heat transfer to the structures is modeled by coupling the CFD equations to 3D heat conduction equations. The spatial discretization of the conservation equations is obtained by a finite element method, the time discretization by a semi-implicit first order incremental projection method.

The generalized mixing length model is used in this study to model turbulence. The user has to define a single length scale l_m and then, the eddy viscosity is computed using:

$$\nu_t = l_m^2 ||S||,\tag{1}$$

where $S = (\nabla u + {}^t \nabla u)/2$ and u stands for the velocity. This length scale corresponds to a filter above which the length scales are resolved and below which the scales are modeled by a turbulent viscosity. With PARs, the selected mixing length is half the PAR exit height.

1.2 PAR model description

In the case of severe accident in a nuclear power plant, hydrogen recombiner allows to decrease the hydrogen density in the containment through a catalytic reaction with oxygen. The oxidation occurs on the recombiner section which is heated by the chemical reaction. Then, it creates a vertical natural convection flow inside the recombiner vessel which supplies the recombiner with hydrogen and oxygen. Hereafter we consider the SIEMENS FR90/1-150 model PAR unit (Figure 1).

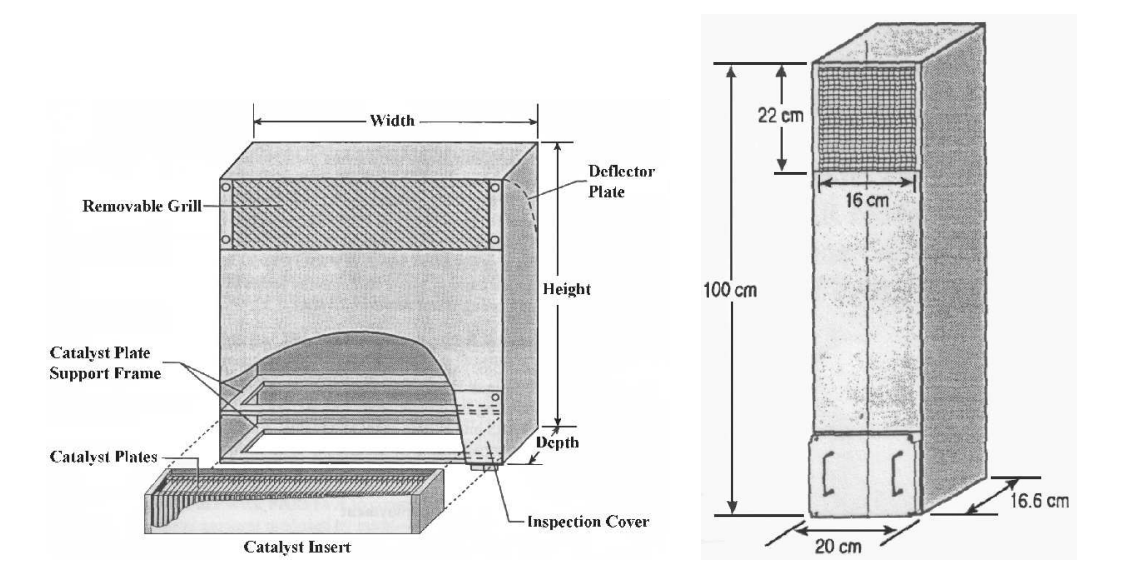


Figure 1: Siemens scale PAR units (left) and FR90/1-150 model PAR unit (right)

To link the PAR black-box model with the CFD formulation we have to evaluate several unknowns: the inlet and the outlet mass flow rates, the inlet and the outlet mass fractions

for each gas component (hereafter, H_2 , O_2 , N_2 and steam), the recombiner plates temperature and the outlet mixture temperature. Accordingly, the system is composed of the following equations [5]: the mass balances for each gas component; the mixture momentum equation; the energy balances for the recombiner plates and the gas mixture.

1.2.1 Mass balance

The mass balance within the recombiner is given by:

$$\frac{dm}{dt} = \dot{m}^i - \dot{m}^o, \tag{2}$$

with m the recombiner gas mass; \dot{m}^i the inlet mass flow rate and \dot{m}^o the outlet mass flow rate. We neglect the recombiner gas mass variation over a time step. Hence the inlet mass flow rate and the outlet mass flow rate are equal $(\dot{m}^i = \dot{m}^o = \dot{m})$ and we obtain for each gas component mass fraction:

$$Y_{N_2}^o = Y_{N_2}^i,$$
 (3)

$$Y_{H_2}^o = Y_{H_2}^i - \frac{\dot{\omega}}{\dot{m}},\tag{4}$$

$$Y_{O_2}^o = Y_{O_2}^i - \frac{M_{O_2}}{2M_{H_2}} \frac{\dot{\omega}}{\dot{m}}, \tag{5}$$

$$Y_{H_2O}^o = Y_{H_2O}^i + \frac{M_{H_2O}}{M_{H_2}} \frac{\dot{\omega}}{\dot{m}}, \tag{6}$$

with M_j the component j molar mass; Y_j^i (resp. Y_j^o) the inlet (resp. outlet) mass fraction of component j; \dot{m} the recombiner mass flow rate and $\dot{\omega}$ the hydrogen consumption mass flow rate of the catalytic reaction.

1.2.2 Momentum equation

We assume that the gaseous mixture is at rest all around the recombiner and the flow steady inside the recombiner. We also suppose that, the temperature and the gas composition are constant in the recombiner, the head loss along the chimney is negligible compared to the head loss at the chimney exit. Then the momentum equation (Bernoulli law) is:

$$\left(K^{i} + k \frac{L}{D_{h}} + K^{o}\right) \frac{1}{2} \frac{\dot{m}^{2}}{\overline{\rho}s^{2}} = g\left((\rho_{ext} - \overline{\rho})L + (\rho_{ext} - \rho^{o})L_{ch}\right), \tag{7}$$

with L the recombiner section length; L_{ch} the chimney length over the recombiner section; $\overline{\rho} = (\rho^i + \rho^o)/2$ the "averaged" gas density within the recombiner section; ρ_{ext} the "averaged" gas density outside the recombiner $(\rho_{ext} = \rho^i)$; K^i the inlet singular pressure loss coefficient; k the regular pressure loss coefficient; k the outlet singular pressure loss coefficient; k the free cross section in the recombiner section and k the flow path diameter in the recombiner section.

1.2.3 Energy balance

We assume that the recombiner housing does not exchange heat with either the gas mixture or the catalytic plates section. The chemical reaction energy is used to heat the recombiner section. Part of this energy heats up the plates while the remaining is given to the gas. Thus, we obtain the following equation to evaluate the plates temperature:

$$\dot{\omega}\Delta H = m_s C_{p_s} \frac{dT_s}{dt} + S_s h \left(T_s - T^i \right), \tag{8}$$

with ΔH the specific enthalpy of the hydrogen combustion reaction (120MJ/kg); m_s , C_{p_s} , T_s and S_s , respectively the mass, the heat capacity, the temperature and the surface of the recombiner plates; h the heat exchange coefficient between the catalytic plates and the gas; T^i the inlet gas temperature.

The gas enthalpy increment between the PAR inlet and the PAR outlet is equal to the energy given to the gas by the catalytic plates and the PAR outlet temperature T^o is given by:

$$\dot{m}\overline{C}_p\left(T^o - T^i\right) = S_s h\left(T_s - T^i\right),\tag{9}$$

with $\overline{C}_p = (C_p^i + C_p^o)/2$ the "averaged" gas heat capacity.

1.2.4 Models and correlations

We briefly describe the physical properties and pressure loss calculations used in the recombiner modeling. For densities, we assume that the gas components are perfect gases.

For each component, the specific heat is supposed to be constant and calculated with a temperature of 400 K. Thus, the mixture specific heat is given by:

$$C_p = \sum_{i=1}^{4} C_{p_i} Y_i, \tag{10}$$

with C_{p_i} the i-species specific heat at constant pressure.

Based on i-species viscosity μ_i and thermal conductivity λ_i , the mixture viscosity and the mixture thermal conductivity are given by [6]:

$$\mu = \sum_{i=1}^{4} \left(\frac{X_i \mu_i}{\sum_{j=1}^{4} X_j \varphi_{ij}} \right), \tag{11}$$

$$\lambda = \sum_{i=1}^{4} \left(\frac{X_i \lambda_i}{\sum_{j=1}^{4} X_j \varphi_{ij}} \right), \tag{12}$$

with
$$\varphi_{ij} = \frac{1}{\sqrt{8}} \left(1 + \frac{M_i}{M_j} \right)^{-\frac{1}{2}} \left[1 + \left(\frac{\mu_i}{\mu_j} \right)^{\frac{1}{2}} \left(\frac{M_j}{M_i} \right)^{\frac{1}{4}} \right]^2$$
.

To calculate the consumption hydrogen mass flow rate of the catalytic reaction $\dot{\omega}$, we use the manufacturer (Siemens) correlation [7]:

$$\dot{\omega} = \min(X_{H_2}, 2X_{O_2}, 0.08) (A p + B) \tanh(X_{H_2} - X_{H_2}^0), \tag{13}$$

with A and B coefficients that depend on the recombiner type; p the total pressure; X_{H_2} and X_{O_2} the inlet hydrogen and oxygen molar fractions; $X_{H_2}^0$ a threshold value equal to 0.005. This hydrogen reaction mass flow rate is also limited to the total recombiner mass flow rates for both reactants hydrogen and oxygen:

$$\dot{\omega} \le Y_{H_2}^i \dot{m} \quad \text{and} \quad \dot{\omega} \le \frac{2M_{H_2} Y_{O_2}^i}{M_{O_2}} \dot{m}.$$
 (14)

For pressure loss coefficient according with [8] we have at the inlet $K^i = 1$ and at the outlet $K^o = 2$. Assuming that the flow inside the recombiner is laminar, the pressure loss coefficient k is calculated by (Hagen-Poiseuille):

$$k = \xi \frac{64}{Re} = \xi \frac{64s\mu}{\dot{m}D_h},\tag{15}$$

with Re the Reynolds number; ξ a correcting coefficient that depends on the shape of the pipe. Considering a very flattened pipe, $\xi = 1.5$.

The last parameter concerns the heat exchange coefficient between the recombiner section and the gas. We use Elenbaas correlation [9, 10] to calculate the convective heat exchange

coefficient h. The gas mixture physical properties in the following equations are calculated from the inlet conditions.

$$h = \frac{\lambda Nu}{e},\tag{16}$$

$$Nu = \frac{1}{24}Ra^* \left(1 - exp(-\frac{35}{Ra^*})\right)^{0.75}, \tag{17}$$

$$Ra^* = \frac{g\beta(T_s - T^i)e^3}{\alpha\nu} \frac{e}{L},\tag{18}$$

with e the gap between two catalytic plates; Nu the Nusselt number; Ra^* a modified Rayleigh number; g the gravity magnitude; β the gas mixture dilatation coefficient; α the gas mixture heat diffusivity; ν the gas mixture viscosity.

1.2.5 Solution procedure

The system of equations can be simplified. As the plates temperature only depends on inlet conditions, it is first evaluated thanks to the energy balance for recombiner section. After some straightforward substitutions in the Bernoulli equation the mass flow rate \dot{m} is the solution of an algebraic equation with the restricted conditions (14):

$$\frac{3}{2}\dot{m}^2 + \frac{48\mu \ sL}{D_h^2}\dot{m} - \frac{1}{2}(\frac{L}{2} + L_{ch})gs^2\rho^{i\ 2}\left(1 - \frac{1}{\left(1 + \frac{S_sh(T_s - T^i)}{T^i\dot{m}(C_p - a\frac{\dot{\omega}}{\dot{m}})}\right)^2\left(1 - \frac{M^i}{2M_{H_2}}\frac{\dot{\omega}}{\dot{m}}\right)^2}\right) = 0,$$

with
$$a = \frac{1}{2} \left(C_{p_{H_2}} + C_{p_{O_2}} \frac{M_{O_2}}{2M_{H_2}} - C_{p_{H_2O}} \frac{M_{H_2O}}{M_{H_2}} \right)$$
.

Then back substitutions allow us to recover outlet conditions [11].

1.2.6 PAR model validation

The KALI/H2 program aims to validate the SIEMENS recombiner performance in some specific conditions (spray, low oxygen content, etc.). The facility associated with KALI/H2 is a cylindrical steel vessel of $15.6m^3$ [12]. Several tests have been performed in order to study the influence of the initial hydrogen concentration, pressure and temperature on the behavior

of the SIEMENS recombiner (Table 1, left). For the averaged dry hydrogen molar fraction within KALI and for PAR exit flow temperature only small differences are observed whereas computed catalytic plates temperature are 30K higher than the measured one [13, 14].

The H2PAR program aims to study the effect of aerosols on the PAR performances. The facility consists of a double terphane enclosure in a volume of about $7\,m^3$ [15]. Nevertheless several tests have been performed in order to study the behavior of the SIEMENS recombiner (Table 1, right). Some comparison have been performed between calculated and measured data on the averaged dry hydrogen molar fraction within H2PAR, PAR exit flow temperature and catalytic plates temperature. Even general trends are recovered, we observe less accuracy than KALI results.

Moreover, the proposed PAR model was validated by performing the numerical PARIS benchmark presented in the next section.

Test	P	T	X_{H2}	X_{H2O}	X_{air}
001	1.3	30.	2	0	98
005	2.9	110.	5	50	45
006	1.3	30.	4	0	96
008	3.3	35.	4	0	96
009	3.25	115.	4	50	46

Test	P	T	$X_{H2}^{(*)}$	X_{H2O}	X_{air}
E12	1.	85.	6.0	0	100
E13	1.	85.	8.5	58	42
E19	1.	70.	8.5	33	67

Table 1: Initial conditions for selected tests performed in KALI facility (left) and H2PAR facility (right). Pressure in bar, temperature in ${}^{o}C$ and molar fraction in vol%. (*) stands for dry air maximum concentration at the end of the H2 injection.

2 PARIS benchmark and associated new cases

SARNET research activities concern experimental programmes, interpretation work and/or modeling activities in order to reduce uncertainties that are considered of importance for nuclear reactor safety and to consolidate severe accident management plans. The SARNET work package WP12 was dedicated to hydrogen behavior in containment and participants decided to define a numerical benchmark on Passive Autocatalytic Recombiner Interaction Studies (PARIS) in order to check the PAR elevation influence on the hydrogen distribution; study natural convection loop interactions when several PARs are present; compare CFD and LP formulations in such situations.

To limit computational resources and to give partners a basic test case, it was decided to

consider a simple 2D square insulated geometry. Thus, walls will not affect the thermodynamic containment atmosphere evolution (no condensation at the wall and no heat exchange to the wall) [16].

The containment is a H*W rectangular box (Figure 2). Box dimensions are characterized by two parameters: the box to PAR height ratio H/h = 5 and the box aspect ratio W/H = 1. PAR location is defined by its bottom left corner coordinates. Coordinates' origin is at the bottom left corner of the box. For the PARIS benchmark 2 PARs are respectively located at (w, h_{ref}) and $(W - 2w, h_{ref})$ with w the PAR width and $h_{ref} = (H - h)/2$. So the PAR middle height is at the box middle height. The entry PAR flow section is the PAR bottom side and the PAR exit flow is directed toward the center of the box. For new cases, a top and a bottom elevation are considered with $h_{top} = H - w - h$ and $h_{bot} = w$.

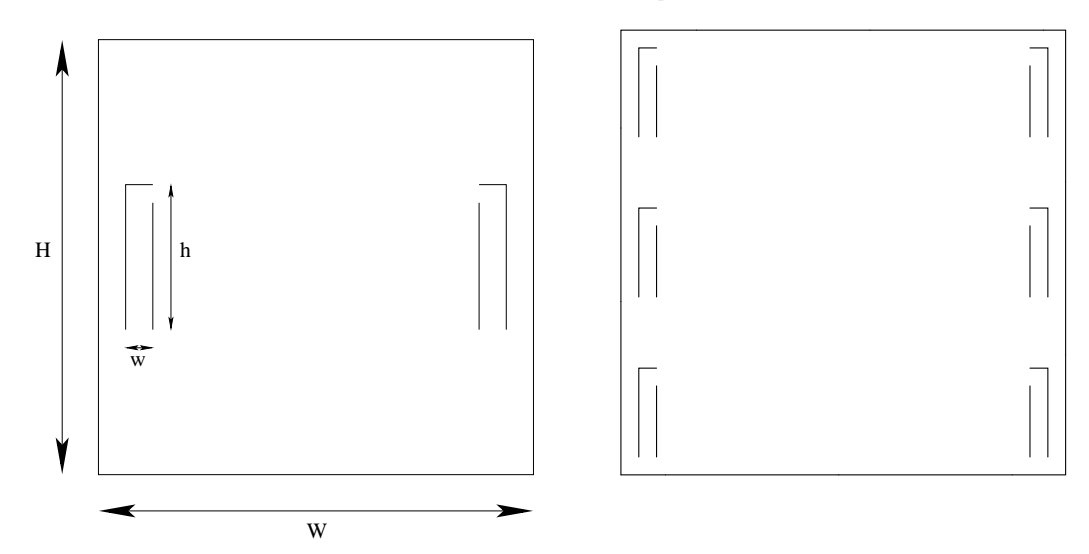


Figure 2: PARIS benchmark definition (left side, not scaled) and PAR locations for the three configurations (right side)

The PAR is a SIEMENS FR90/1-150 like PAR. Hereafter, we consider a PAR height h=1m and a PAR width w equal to the PAR depth (w=0.2m). The entry flow section and the exit flow section are also equal to w. In each PAR 15 catalytic plates are considered. Plate height (resp. depth and width) is 0.15m (resp. 0.15m and 0.0001m). Plates inter-space is 0.01m. The consumption hydrogen rate in kg/s is the SIEMENS law (13) with $A=0.48\times 10^{-8}$ and $B=0.58\times 10^{-3}$.

An initial homogeneous mixture (air, steam and H_2) at $T_1 = 393K$ is considered: the air mass is the one we have at $P_0 = 10^5 Pa$ and $T_0 = 298K$; the hydrogen molar fraction in dry

air X_{h2}^{dry} is 5vol%; steam is at saturation state. Hence the total pressure P_1 is given by:

$$P_1 = P_{sat}(T_1) + \frac{P_{air}}{1 - X_{b2}^{dry}},\tag{19}$$

with $P_{air} = T_1 P_0 / T_0$ and the molar fraction for each species is given by: $X_{air} = P_{air} / P_1$, $X_{h2o} = P_{sat}(T_1) / P_1$ and $X_{h2} = X_{h2}^{dry} (1 - X_{h2o})$.

As the containment is insulated, there are no mass and no energy fluxes through the wall. For the velocity, no-slip boundary conditions are assumed. The prescribed boundary conditions have to be applied for all the transient of 3000s.

3 Comments and analysis

For all cases, numerical choices are identical to the PARIS benchmark one's [17]. We choose a linear interpolation for the velocity and element piecewise constant pressure. In order to verify a numerical stability condition associated with velocity-pressure compatibility (the so-called inf-sup or LBB condition) MACRO-element stabilization is used. A regular 200*200 square element mesh is used. The number of element along the PAR height (resp. along the PAR width) is 40 (resp. 8). From 0 to $60 \, s$ the time step is constant and equal to $0.1 \, s$. Later on, it is set to $0.5 \, s$. For turbulence modeling, the generalized mixing length model is used in this study. The mixing length we used is based on half the PAR exit height. Hence it is $0.1 \, m$.

3.1 Mid-elevation results

This elevation corresponds to the PARIS benchmark situation. According with the PARIS benchmark results, three layers have been identified [17]: a floor layer with low mass and thermal mixing processes where hydrogen concentration and temperature are not so affected with PAR efficiency. A roof layer with high mass and thermal mixing processes where hydrogen depletion is very fast and already effective after 300s. A one meter depth buffer layer with high vertical hydrogen concentration and temperature gradients in order to join the floor layer and the roof layer.

Accordingly, it comes out three characteristic times. The shorter is an hydrogen depletion time when most of the hydrogen located in the roof layer is burnt. PAR inlet suction

The 14^{th} International Topical Meeting on Nuclear Reactor Thermalhydraulics, NURETH-14 Toronto, Ontario, Canada, September 25-29, 2011.

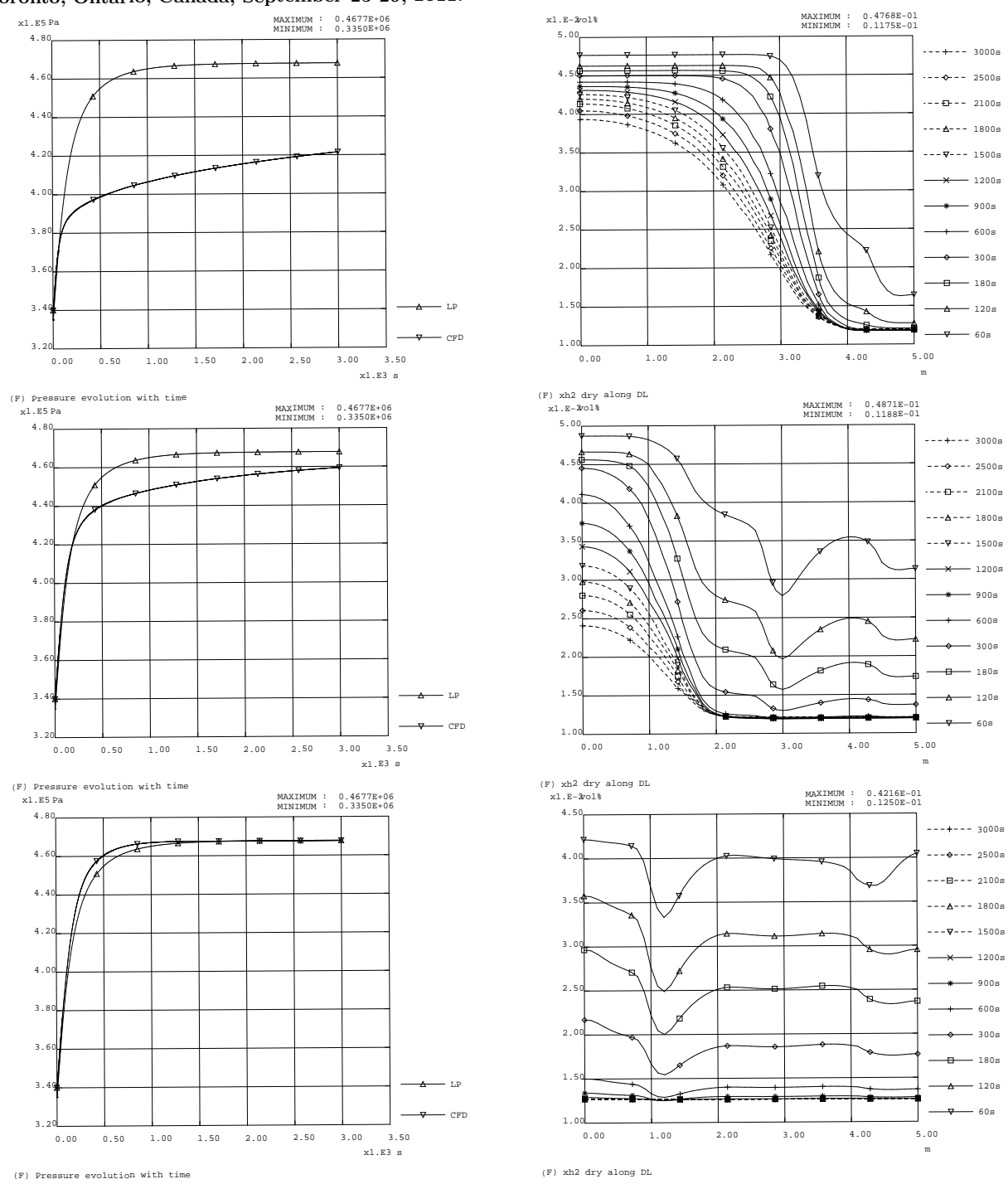


Figure 3: Pressure evolution with time (left) and molar hydrogen fraction in dry air along the vertical line x=2w at several times (right) when PARs are located at the top (top), middle (middle) or bottom (bottom) elevation.

and PAR exit blowing make the flow moving. Then a roof layer time when inertia effects decrease and a constant temperature and hydrogen mass roof layer develops. At least a diffusion process time. If PAR inlet belongs to the buffer region, it characterizes mixing process at the interface between the buffer layer and the roof layer (due to no flow in the PAR). If not, it characterizes mixing process at the interface between the buffer layer and the floor layer.

It is illustrated Figure 3 (right side, middle graphic) where we plot the dry hydrogen molar fraction along the vertical line x = 2w at several times (the abscissa 0 corresponds to the floor; 5 to the roof); Figure 4 where we plot the velocity and X_{H2}^{dry} at t = 600s.

3.2 Top and bottom elevation results

The effect of the PAR elevation is clearly shown on Figure 4: the higher the PAR is located along the vertical wall, the smaller the convection loop associated with the PAR is and the larger the floor layer is. Hence after ten minutes only a residual hydrogen consumption rate is visible when PARs are located at the top elevation while PARs continue to burn the residual floor layer when located at the bottom.

It is also interesting to compare the pressure given by the CFD and the LP approaches (Figure 3, left side). LP pressure evolution with time indicates the fastest process we can observe as the mixture in this model is continuously perfectly mixed — we only use one cell to describe the cavity. Hence, a single volume lumped parameter model is not able to take into account any stratification. So the closer the CFD and LP pressures are, the lower the depth of the stratified area is. It's why the same steady state is only reached when PARs are located at the bottom of the facility. The largest difference appears when PARs are located at the top due to the unburnt 3 meters floor layer depth.

Conclusion

Even though PARIS configuration is simple, some interesting features appear.

In the situation we are dealing with (a five meters square isolated volume with a 5 vol% hydrogen, saturated steam and air homogeneous mixture initially at rest) we observe hydrogen mass and thermal stratification when PARs are moving toward the top of the box: the higher the PAR is located along the vertical wall, the smaller the convection loop associated with the PAR is and the larger the floor layer is.

The 14^{th} International Topical Meeting on Nuclear Reactor Thermalhydraulics, NURETH-14 Toronto, Ontario, Canada, September 25-29, 2011.

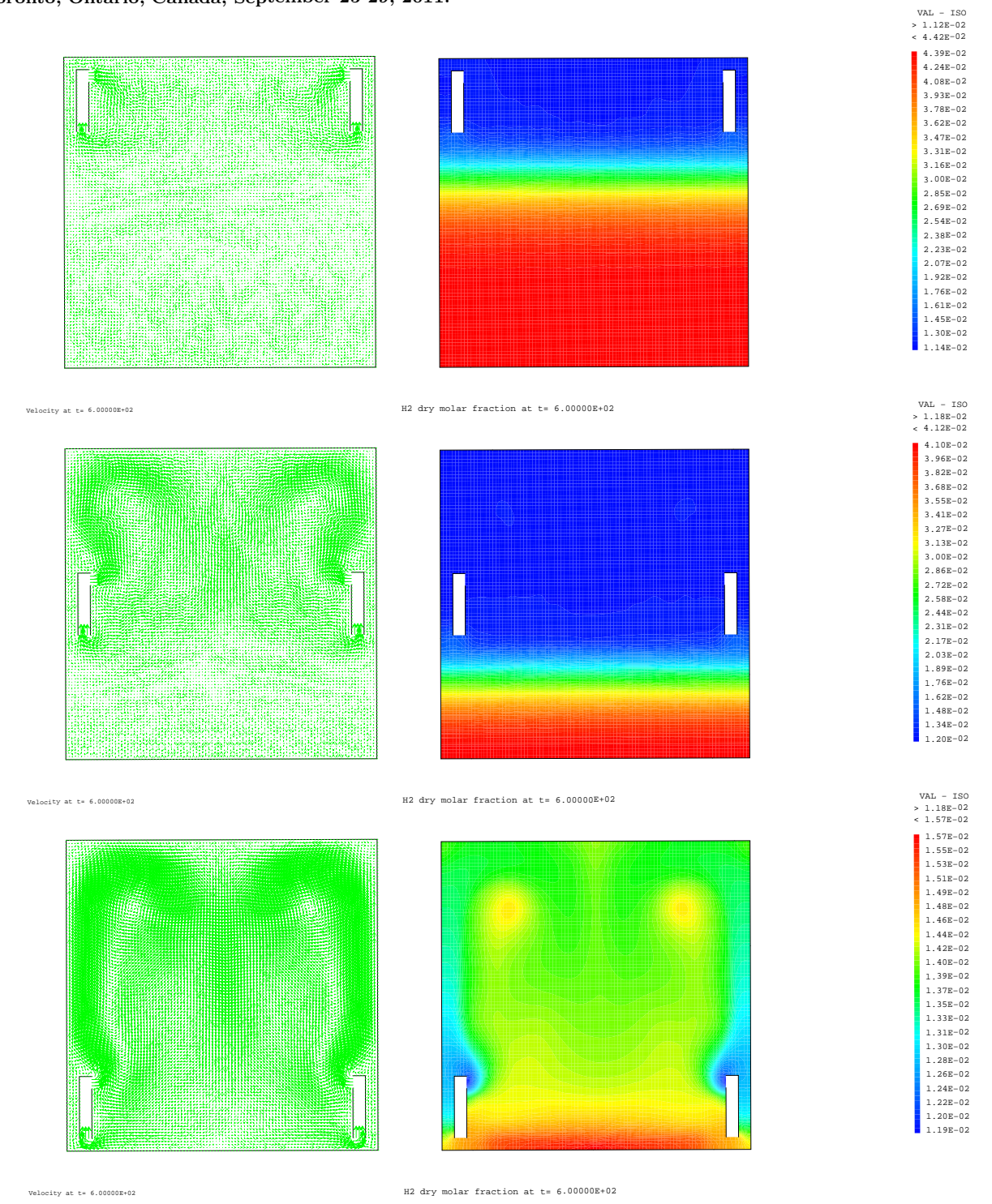


Figure 4: Velocity (left) and molar hydrogen fraction in dry air (right) at t = 600s.

It is clear that floor layer stability depends on wall boundary conditions [18] and bidimensional geometry enhanced artificially inertial effects but PARIS configuration illustrates that other processes than PAR suction and blowing effects are necessary to mobilize the floor layer. So stratification stability with scenarios close to real situations have to be addressed. It is planned to perform in 2013 some specific tests in the MISTRA facility of CEA [19] to illustrate the ability of PAR devices to mobilize the atmosphere below the PAR.

References

- [1] S. Kudriakov, F. Dabbene, E Studer, A. Beccantini, J.-P. Magnaud, H. Paillère, A. Bentaïb, A. Bleyer, J. Malet, E. Porcheron, and C. Caroli. The TONUS CFD code for hydrogen risk analysis: Physical models, numerical schemes and validation matrix. *Nuclear Engineering and Design*, 238:551–565, 2008.
- [2] A. Beccantini, E Studer, S. Gounand, J.-P. Magnaud, T. Kloczko, C. Corre, and S. Kudriakov. Numerical simulations of a transient injection flow at low Mach number regime. *International Journal for Numerical Methods in Engineering*, 76:662–696, 2008.
- [3] A. Beccantini and E. Studer. The reactive Riemann problem for thermally perfect gases at all combustion regimes. *International Journal for Numerical Methods in Fluids*, 64:269–313, 2010.
- [4] R.B. Bird, W.E. Stewart, and E.N. Lightfoot. Transport phenomena. Wiley ed, 1960.
- [5] P. Berne. Recombineur catalytique d'hydrogène, proposition de modèle simple. Rapport d'étude SERAC/LESI/96-11, IRSN, 1996.
- [6] C.R. Wilke. A viscosity equation for gas mixtures. The Journal of Chemical Physics, 18:517–519, 1950.
- [7] M. Mohaved. Recombiner model for lumped parameter codes validation and application. Work report KWU NA-M/95/E054, SIEMENS, 1995.
- [8] I.E. Idel'cik. Mémento des pertes de charge. Editions Eyrolles, 1969.
- [9] W. Elenbaas. Heat dissipation of parallel plates by free convection. *Physica*, 1942.
- [10] P. Teertstra, J.R. Culham, and M.M. Yovanovitch. Comprehensive review of natural and mixed convection heat transfer models for circuit board arrays. *J. of Electronics Manufacturing*, 7:79–92, 1997.

- The 14th International Topical Meeting on Nuclear Reactor Thermalhydraulics, NURETH-14 Toronto, Ontario, Canada, September 25-29, 2011.
- [11] F. Dabbene. Modélisation d'un recombineur catalytique par une approche 0D, 2010. CEA internal report SFME/LTMF/RT/10-018/A.
- [12] G. Avakian, L. Averlant, and O. Braillard. Hydrogen mitigation by a SIEMENS recombiner in KALI facilities. *Topical Meeting on Research Facilities for the Future of Nuclear Energy*, 1996.
- [13] P. Zavaleta. Validation du modèle recombineur du code TONUS, 1ère partie: Calcul des essais KALI/H2. Rapport d'étude DPEA/SERAC/LPMC/98-20, IPSN, 1998.
- [14] P. Zavaleta. Validation du modèle recombineur du code TONUS, 2ème partie: Calcul des essais H2PAR et KALI/H2. Rapport d'étude DPEA/SERAC/LPMAC/99-13, IPSN, 1999.
- [15] D. Leteinturier. Essais H2PAR: période mi-98 à fin 2000, synthèse des essais et conclusions du programme. Rapport d'étude DPEA/DIR/02/01, IRSN, 2002.
- [16] H. Wilkening, I. Kljenak, W. Ambrosini, A. Bentaib, L. Blumenfeld, F. Dabbene, J. Malet, E-A. Reinecke, E. Takasuo, and J.R. Travis. European research on issues concerning hydrogen behaviour in containment within the SARNET network of excellence. In *Proc. of Int. Congress on Advances in Nuclear Power Plants (ICAPP '08)*. Anaheim(CA), USA, June 8-12, 2008.
- [17] F. Dabbene and P. Paillère. Paris benchmark results, 2007. SARNET report, SARNET-CONT-P04 (also CEA internal report SFME/LTMF/RT/07-003/A).
- [18] E-A. Reinecke, A. Bentaïb, S. Kelm, W. Jahn, N. Meynet, and C. Caroli. Open issues in the applicability of recombiner experiments and modelling to reactor simulations. *Progress in Nuclear Energy*, 52:136–147, 2010.
- [19] I. Tkatschenko, E. Studer, J-P. Magnaud, L. Blumenfeld, H. Simon, and H. Paillère. Status of the mistra programme for the validation of containment thermal-hydraulic codes. In Proc. of 11th Int. Topical Meeting on Nucl. React. Thermalhydraulics, NURETH-11. Avignon, France, October 2-6, 2005.